Sound radiation from nested cylindrical shells

Hongjian Wu[1]; Herwig Peters[1]; Nicole Kessissoglou[1]

[1] School of Mechanical and Manufacturing Engineering, UNSW Australia, Sydney NSW 2052

ABSTRACT

Fluid-loaded nested cylindrical shells are modelled using a doubled-walled cylindrical shell structure closed at each end by circular end plates and excited by a transverse force at one end. The effects of various influencing factors on the radiated sound power are examined corresponding to non-concentricity of the cylindrical shells, entrained fluid and rib connections in the annular space between the inner and outer shells. The doubled-walled cylindrical shell is modelled using two different approaches to consider low and high frequencies. In the first approach, a fully coupled finite element/boundary element model of the fluid-loaded nested cylindrical shells is developed, whereby the finite element method is used to model the structure and the boundary element method is used to model the entire fluid domain. The second approach uses an energy based method to consider the high frequency range. A hybrid finite element/statistical energy analysis technique is developed whereby the rigid components corresponding to the annular ribs and end plates are modelled using finite elements, while the fluid and flexible shell structures are modelled using statistical energy analysis. Results obtained using the deterministic and statistical numerical methods are compared.

Keywords: Nested cylindrical shells, finite element analysis, boundary element analysis, sound power
I-INCE Classification of Subjects Number(s):75.2, 75.3, 75.5

1. INTRODUCTION

Vibro-acoustic analyses of underwater structures may be conducted analytically (1, 2) and numerically (3) as a coupled fluid-structure interaction problem. An underwater structure can be generally idealised as a ring stiffened cylindrical shell subject to external water loading (4, 5). Many previous studies on fluid-loaded cylindrical shells are concerned with single wall cylinders, with few studies on the vibro-acoustic characteristics of double-walled cylinders. Lee and Kim (6) developed an analytical model of two concentric cylindrical shells of infinite length based on Love's equations. They showed that the double-walled shell with a large air-gap provides good noise insulation. Fourier transform techniques were used by Skelton (7, 8) to predict the scattered pressure from two concentric infinite cylindrical shells linked by rigid annular ribs. Balena et al. (9) examined noise reduction of single and double-wall cylinders using a range of stiffeners. Below the cylinder ring frequency, ring stiffeners can be modelled using a smeared approach. However this smeared approach is not suitable at frequencies above the ring frequency. The entrained fluid in the annular space between concentric submerged cylindrical shells has also been studied theoretically and experimentally (10, 11) where the inner and outer cylindrical shells are shown to be acoustically connected by the entrained fluid.

At high frequencies, structural wavelengths become very small thus requiring very small element sizes in either a finite element or boundary element model. Deterministic methods are generally limited to the low frequency range. Statistical energy analysis (SEA) (12) is an energy based method to overcome the limitations of deterministic methods at higher frequencies. Using SEA for fluid-structure interaction problems, the surrounding fluid is considered to be an additional subsystem in an SEA model. The validity of the SEA equations is usually limited to high frequencies because of the underlying assumptions of high modal overlap and weak coupling between structural subsystems. In the mid-frequency range, the dynamic behaviour of a structure is the combination of long wavelength global modes and short wavelength local modes. An emerging approach to predict mid frequency vibro-acoustic responses is the hybrid finite element-statistical energy analysis (FE-SEA) method (13, 14).

In this paper, a coupled finite element/boundary element (FE/BE) method as well as a hybrid FE-SEA method are used to numerically model fluid-loaded nested cylindrical shells subject to a transverse point force. Numerical results in the low frequency range are initially presented to examine the effects of various

[1] hongjian.wu@student.unsw.edu.au

influencing factors on the radiated sound power of the nested shells such as the entrained fluid in the annular space between the inner and outer shells, non-concentricity of the shells, and annular ribs linking the inner and outer cylindrical shells. A comparison of the radiated sound power obtained from the deterministic and statistical methods is also presented.

2. MODEL DESCRIPTION

A schematic diagram of fluid-loaded nested cylindrical shells is shown in Figure 1. The system consists of two concentric cylindrical shells of different thickness, connected together by circular end plates and annular ribs. The inner cylindrical shell contains no fluid. The outer cylindrical shell is surrounded by a heavy fluid. The annular space between the inner and outer cylindrical shells is filled with either a heavy or light fluid. The inner and outer cylindrical shells have the same length L and are assumed to be thin-walled, that is, the shell thickness h is much smaller than the mean shell radius R. The shells are closed at each end by circular end plates. The shells are further connected with three evenly spaced annular plates. Both cylindrical shells are of steel with material parameters denoted by Young's modulus E, Poisson's ratio υ and density ρ. The physical parameters and material properties for the structure and fluid are listed in Table 1. In the analysis, the Young's modulus of the circular end plates and annular ribs is set as either 210 or 210,000 GPa. The more realistic domed end closures in practical applications of fluid-loaded cylinders are much stiffer than the flat ends used here. For this reason, the stiffness of the circular end plates has been increased to avoid the relatively flexible end plates.

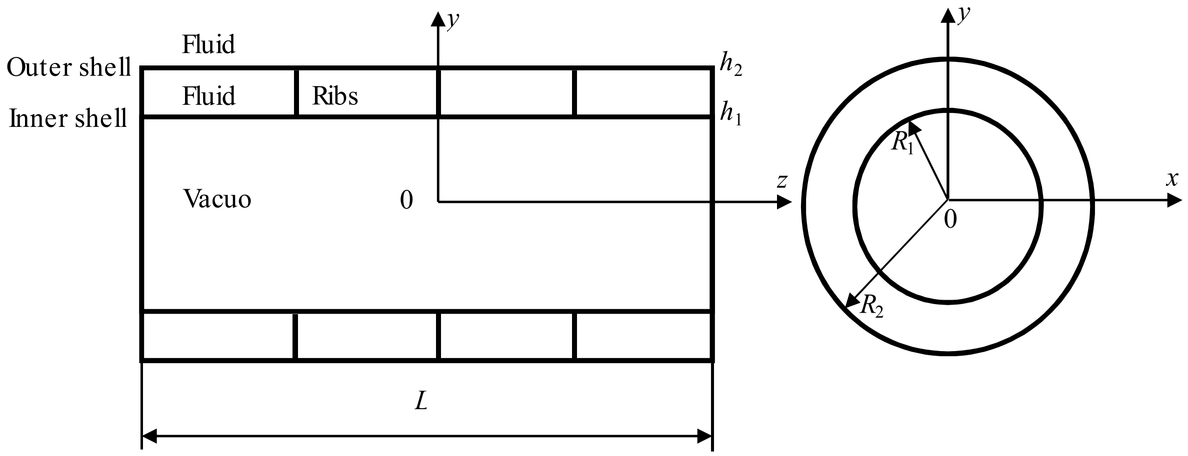

Figure 1 – Schematic diagram of the concentric nested cylindrical shells

Table 1 – Physical parameters and material properties of the nested cylindrical shells

Parameter	Inner shell	Outer shell	End plates	Ribs	Air	Water
Radius	R	$1.25R$	$1.25R$	-	-	-
Thickness	h	$0.6h$	$0.1h$, h	h	-	-
Length	L=12R	L=12R	-	-	-	-
Density ρ (kg/m^3)	7860	7860	7860	7860	1.204	1000
Sound speed c (m/s)	5960	5960	5960	5960	343	1500
Young's modulus E (GPa)	210	210	210, 210E3	210, 210E3	-	-
Poission's ratio υ	0.3	0.3	0.3	0.3	-	-

3. NUMERICAL MODEL

3.1 Finite element/boundary element model

A fully coupled FE/BE model is achieved by imposing a continuity condition of the fluid particle and structural node normal velocity on the fluid-structure interface, as well as an equilibrium condition of the acoustic pressure acting normally on the structural surface. Assuming a time harmonic dependence, the dynamic equilibrium equation for an elastic structure is given by (15)

$$\mathbf{M}\ddot{\mathbf{q}} + \mathbf{C}\dot{\mathbf{q}} + \mathbf{K}\mathbf{q} = \mathbf{f} \tag{1}$$

where $\mathbf{M}$ is the global mass matrix, $\mathbf{C}$ is the global damping matrix and $\mathbf{K}$ is the global stiffness matrix. $\ddot{\mathbf{q}}$, $\dot{\mathbf{q}}$ and $\mathbf{q}$ are the nodal acceleration, velocity and displacement vectors, respectively. $\mathbf{f}$ is the external force vector. Using the mode superposition principle, the finite element nodal point displacements can be obtained as

$$\mathbf{U}(t) = \sum_{i=1}^{m} \Phi_i x_i(t) \tag{2}$$

where $\mathbf{U}$ is the vector of nodal point displacements, Φ_i is the i^{th} modeshape vector, x_i is the i^{th} mode displacement, m is the total number of modes, and t is the time variable. Structural damping was incorporated into the numerical model using proportional damping. The proportional damping model expresses the damping matrix as a linear function of the mass and stiffness matrices as follows (16)

$$\mathbf{C} = \alpha\mathbf{M} + \beta\mathbf{K} \tag{3}$$

where α and β are real scalars. In this work, the effect of varation in damping of the outer cylindrical shell on the radiated sound power was conducted by setting pre-determined constants of α and β in equation (3). The proportional damping model considers that the structural damping ratio is a linear superposition of the mass and stiffness proportional damping effects. The proportional damping ratio ξ_i for the i^{th} mode is calculated as (17)

$$\xi_i = \frac{\alpha}{2\omega} + \frac{\beta\omega}{2} \tag{4}$$

where ω is the radian frequency.

The indirect boundary element method was used to calculate the acoustic field as it simultaneously calculates the responses of the external fluid and the entrained fluid between the cylindrical shells. The acoustic pressure jumps and structural displacements of a coupled FE/BE model are obtained by (18)

$$\begin{bmatrix} \mathbf{K} - \omega^2\mathbf{M} & \mathbf{C}_g^{\mathrm{T}} \\ \rho\omega^2\mathbf{C}_g & \mathbf{H} \end{bmatrix} \begin{bmatrix} \mathbf{u}_s \\ \mathbf{p}_j \end{bmatrix} = \begin{bmatrix} \mathbf{f}_s \\ \mathbf{f}_f \end{bmatrix} \tag{5}$$

where $\mathbf{f}_s$ and $\mathbf{f}_f$ are respectively the nodal structural forces and forces due to fluid loading acting on the surface of the structure, $\mathbf{u}_s$ is the nodal displacement of the structure, $\mathbf{p}_j$ is the vector of nodal values of acoustic pressure jumps, $\mathbf{C}_g$ is the geometrical coupling matrix and $[\cdot]^{\mathrm{T}}$ denotes the transpose matrix operator. $\mathbf{H}$ is the frequency dependent indirect boundary element influence matrix.

The nested cylindrical shells were initially modelled with 3584 QUAD 8 shell elements (32 elements in the circumferential direction and 45 elements in the longitudinal direction) and solved using MSC/Patran/Nastran to obtain the FE mesh and structural modes of the nested cylindrical shells. A proportional damping ratio of

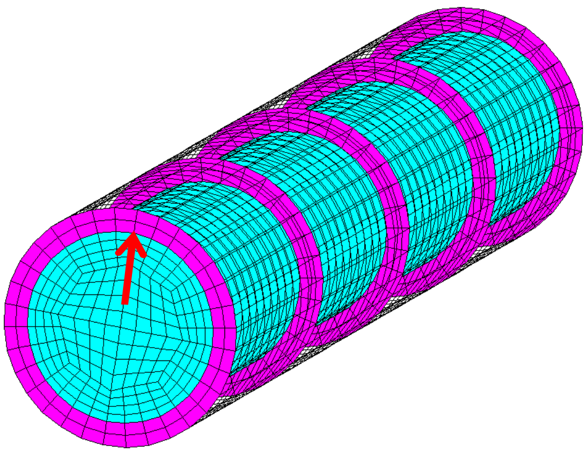

Figure 2 – FE/BE model of the nested cylindrical shells with annular ribs

0.02 was applied to the structural modes of the nested cylindrical shells. A transverse point force was applied at the junction between one end plate and the inner cylindrical shell, as shown in Figure 2. The FE mesh and structural modes were then imported into SYSNOISE to calculate the radiated sound power. The FE structural model and the indirect BEM acoustic model were linked together via a fluid-structure interaction surface and solved from 0.5 to 80 Hz in steps of 0.5 Hz. In the analysis, only the fluid-structure interaction surface of the inner and outer cylindrical shells was considered as the transverse point force predominantly excites the bending modes of the shells. As shown in Figure 1, the fluid loading is applied to both sides of the outer shell which makes the direct BEM unsuitable; the indirect BEM was used. Therefore, no sound radiation from the circular end plates was considered and the end plates only act as transmission paths of vibrational energy between the inner and outer shells. Once the acoustic pressure and normal particle velocity on the radiating surface are known, the total radiated sound power was numerically obtained as (19)

$$\Pi_{\text{num}} = \frac{1}{2}\text{Re}\left\{ \int_{\Gamma} p v^{*} \mathrm{d}\Gamma \right\} \tag{6}$$

where p is the acoustic pressure of the fluid, v is the fluid particle velocity on the wet surface of the structure and Γ is the fluid-structure interface surface area. $[\cdot]^{*}$ denotes the conjugate complex and Re denotes the real part of the complex value. In the proceeding results, the reference sound power is 10^{-12} W.

3.2 Hybrid finite element/statistical energy analysis model

A detailed formulation of the hybrid FE-SEA methodology can be found in Refs. (13, 14). In what follows, a brief introduction on the fundamental theory is presented. The key idea in the hybrid FE-SEA method is that in any complex mechanical system, there exists a middle frequency range in which some subsystems of low modal density will exhibit modal behavior while other subsystems of high modal density exhibit diffuse behaviour. Therefore, the complex mechanical system is represented as an assembly of deterministic FE components known as the master system and an assembly of SEA subsystems with uncertain properties. The power balance equation for subsystem i is given by (12)

$$P_i = \omega \eta_i E_i + \omega \sum_{j \neq i} \eta_{ij} n_i \left(\frac{E_i}{n_i} - \frac{E_j}{n_j} \right) \tag{7}$$

where n_i , η_i are respectively the modal density and loss factor of subsystem i. η_{ij} is the coupling loss factor between subsystems i and j. The input power P_i and subsystem energies E_i, E_j are averaged over ensemble properties or frequency. To couple the FE and SEA methods, the hybrid FE-SEA equation can be derived as (13, 14)

$$P_i + P_{in,i}^{ext} = \omega(\eta_i + \eta_{d,i}) E_i + \omega \sum_{j \neq i} \eta_{ij} n_i \left(\frac{E_i}{n_i} - \frac{E_j}{n_j} \right) \tag{8}$$

Compared with the standard SEA equation given by equation (7), the hybrid FE-SEA equation has two additional terms: (i) a contribution $P_{in,i}^{ext}$ to the input power arising from forces applied directly to the master system; (ii) the additional loss factor $\eta_{d,i}$ of the master system. These two additional terms can be expressed analytically as a function of the total dynamic stiffness matrix and the cross-spectral density matrix of the external load applied to the master system.

The nested cylindrical shells with annular ribs were modelled using the Hybrid FE-SEA module in the VA-One software (20), as shown in Figure 3. The rigid end plates and annular ribs are of low modal density and therefore modelled as FE subsystems while the inner and outer cylindrical shells were modelled as SEA subsystems. The water was modelled as a semi-infinite-fluid (SIF) subsystem. The fluid load was applied to the outer surface of the structure by connecting the SIF subsystem to the SEA subsystems of the inner and outer cylindrical shells and the circular end plates. A transverse point force excitation was applied at the same location as in Figure 2.

4. NUMERICAL RESULTS

In the numerical results, the nested cylindrical shells are surrounded by heavy fluid. Heavy fluid is also considered in the annular space between the inner and outer shells in all cases except for Figure 4, which compares results for the case of entrained water with that of entrained air. To simulate strong coupling between the inner and outer shells, the Young's modulus of the circular end plates was increased to 210E3 GPa, corresponding to a value 1000 times greater than the normal value for steel. The annular ribs are only included in the models for the results presented in Figures 9 and 13.

4.1 Entrained Fluid Loading

The entrained fluid connects the inner and outer shells of the nested cylindrical shells acoustically due to the fluid-structure coupling. The inner and outer shells are mechanically connected by the rigid circular plates at each end. The radiated sound power from the nested cylindrical shells entrained with a heavy or light fluid is presented in Figure 4. The resonant peaks in the radiated sound power correspond to successive circumferential bending modes of the cylindrical shells. Comparison of the radiated sound power for the two cases of entrained fluid shows that the fluid in the annular space between the two cylindrical shells has a significant effect on the resonant peaks. For the case of entrained water, there is a decrease in the resonant frequencies due to the added dynamic mass of entrained water loading. A reduction in the radiated sound power at the first three bending modes is attributed to additional radiation damping provided to the acoustic radiation modes of the nested cylindrical shells by the entrained water. For the case of entrained air, an increase in modal density with increasing frequency is observed as a greater number of short wavelength, high order local modes of the inner and outer shells are excited.

4.2 Proportional Damping

The effect of structural damping on the radiated sound power from the nested cylindrical shells was examined by varying the proportional damping coefficients corresponding to the mass damping coefficient α and the stiffness damping coefficient β in equation (3). Using the procedure described in ref. (17), the proportional damping coefficients were calculated for two values of the frequency-dependent proportional damping ratios using equation (4), at frequencies of 5 and 80 Hz which covers the frequency range for the results in this work. The two selected damping ratios and corresponding calculated damping coefficients are listed in Table 2. Figure 5 shows that the resonant peaks in the radiated sound power are reduced with an increase in damping. Little reduction in the peak radiated sound power occurs below 20 Hz. The effect of damping on the peak radiated sound power increases with increasing frequency.

Table 2 – Proportional damping ratios and coefficients

Damping ratio	α	β
0.02	1.18	7.49E-5
0.04	2.37	1.50E-4

4.3 Non-Concentricity

The influence of non-concentricity of the cylindrical shells on the radiated sound power is examined by varying the non-concentricity parameter d, shown in Figure 6. From Figure 7, it is observed that the influence of non-concentricity is essentially negligible if d/R is small. This finding is also demonstrated from the analytical solution of Shaw (21).

4.4 Annular Ribs

In Figure 8, the annular space between the inner and outer shells is divided into four compartments by three evenly spaced annular ribs. The physical parameters of the annular ribs are listed in Table 1. Whilst the FEM model was modified to include the annular ribs, the same BEM model was used for the calculation of the radiated sound power for both the ribbed and unribbed nested cylindrical shells, corresponding to the BEM model for the unribbed shells.

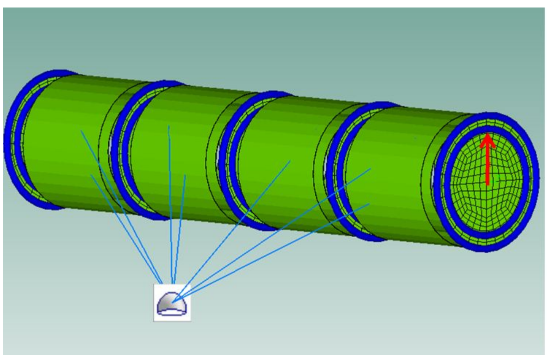

Figure 3 – Hybrid FE-SEA model of the nested cylindrical shells with annular ribs

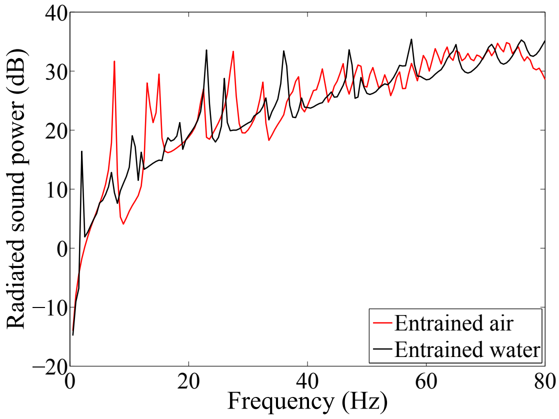

Figure 4 – Radiated sound power for different entrained fluid in the annular space

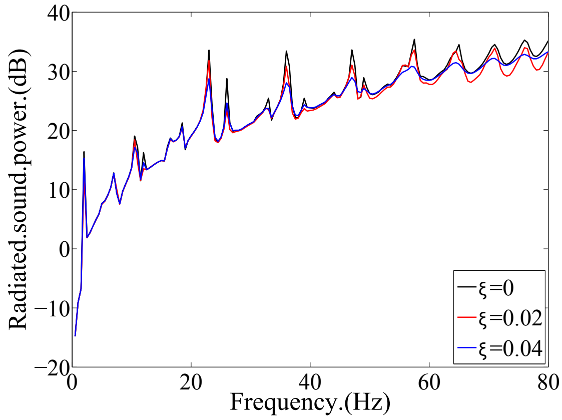

Figure 5 – Radiated sound power for different proportional damping ratios

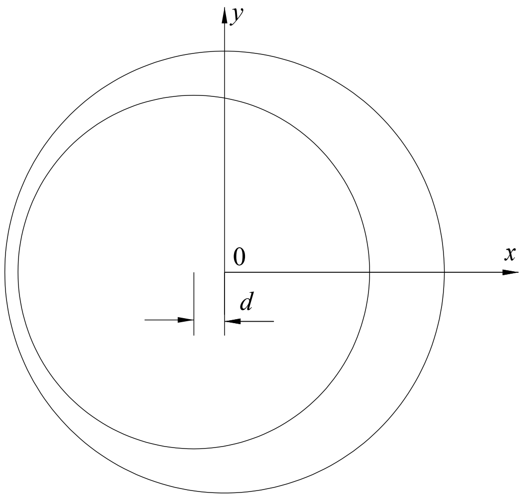

Figure 6 – Definition of the non-concentricity parameter in the non-concentric nested cylindrical shells

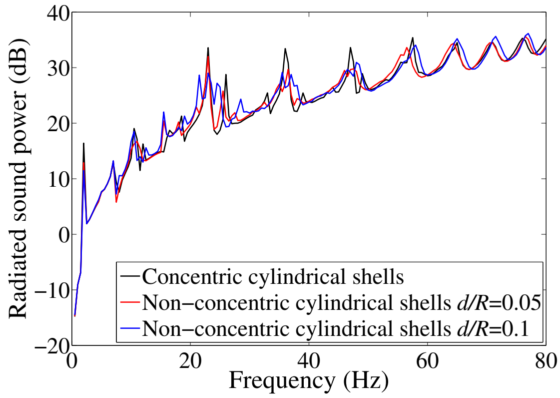

Figure 7 – Radiated sound power from the concentric and non-concentric nested cylindrical shells

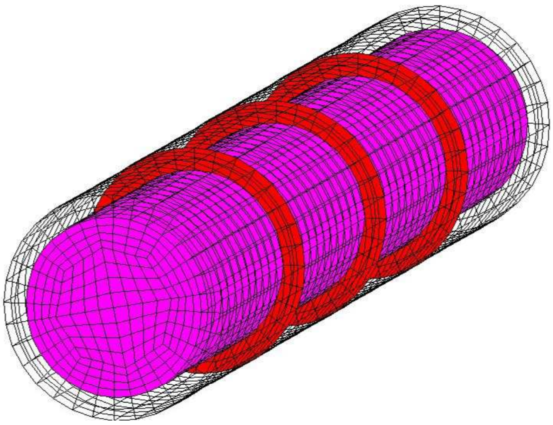

Figure 8 – Structural and acoustic mesh of the nested cylindrical shells with annular ribs

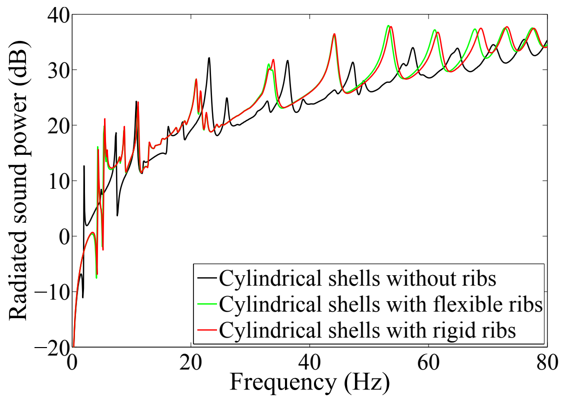

Figure 9 – Radiated sound power from the nested cylindrical shells with and without annular ribs

Figure 9 compares the radiated sound power for unribbed nested cylindrical shells and the shells with either flexible or rigid annular ribs. It is observed that the resonant frequencies of the shell bending modes are increased by adding annular ribs to the nested cylindrical shells, which is attributed to the increased bending stiffness of the cylindrical shells. The effect of rigid annular ribs compared to flexible ribs on the radiated sound power is not significant. Hence, the stiffness of the annular ribs does not significantly affect the vibrational characteristics of the cylindrical shells.

4.5 Circular End Plates

The effect of thickness and stiffness of the circular end plates on the radiated sound power is examined as follows. Figures 10 and 11 respectively present the radiated sound power of the nested cylindrical shells closed with circular end plates with varying thickness and stiffness. In Figure 10, the Young's modulus of the rigid end plates is kept constant at 210E3 GPa and the thickness of the end plates is reduced from 40 to 4 mm. In Figure 11, the thickness of the end plates is kept constant at 40 mm and the Young's modulus is reduced from 210E3 to 210 GPa. If the thickness of the end plates is negligible or if the stiffness of the end plates is very low, the inner and outer shells vibrate independently and are only acoustically connected by the entrained fluid in the annular space. Increasing the flexibility of the end plates by either reducing the thickness or elasticity results in an increase in radiated sound power. This is attributed to the fact that the cylindrical shells are less constrained by the rigidity of the end plates and as such are able to vibrate more freely, resulting in greater structure-borne radiated sound.

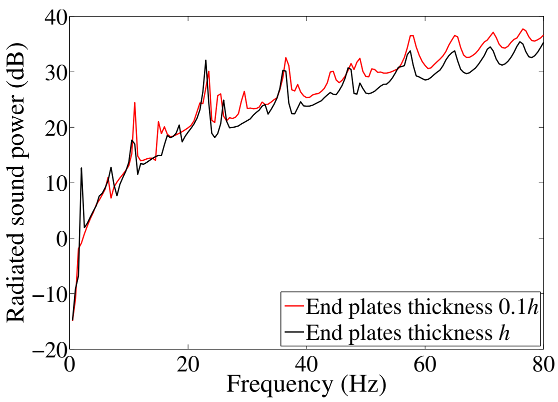

Figure 10 – Radiated sound power from the nested cylindrical shells with varying end plate thickness

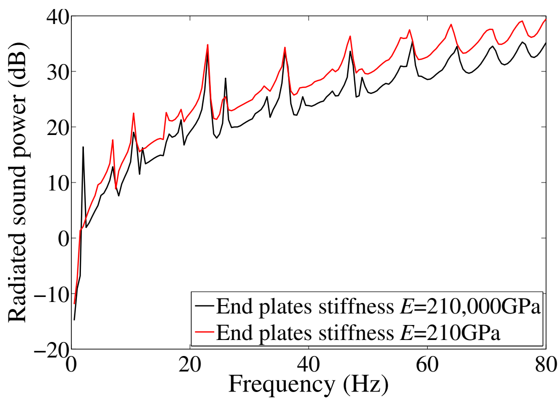

Figure 11 – Radiated sound power from the nested cylindrical shells with varying end plate stiffness

4.6 Deterministic and Statistical Models

Figures 12 and 13 present the radiated sound power from the nested cylindrical shells with and without rigid annular ribs using both coupled FE/BE and hybrid FE-SEA methods. Below 80 Hz, the discrete peaks in the coupled FE/BE results correspond to the bending modes of the cylindrical shells which cannot be predicted by the hybrid FE-SEA models due to the inherent averaging process of the modal energy in the frequency domain. At lower frequencies, the radiated sound power predicted by the hybrid FE-SEA models is considered to be less accurate than the radiated sound power predicted deterministically as there is not a sufficient number of structural modes. Using coupled FE/BE, the mesh size should be proportional to the frequency of the problem in order to have a more accurate solution. For frequencies above 80 Hz, the mesh size of coupled FE/BE models in this work was increased from 3584 to 7124 elements (48 elements in the circumferential direction and 90 elements in the longitudinal direction), which is the maximum model size possible given the available computational resources. It is observed that the difference in the sound power level between the coarse and finer mesh is not very significant in the frequency range between 80 and 120 Hz which indicates that the mesh discretisation may be sufficient up to 250 Hz. The maximum radiated sound power occurs close to the ring frequency of the nested cylindrical shells. Reasonable agreement in the trend for the radiated sound power is observed between the deterministic and statistical numerical techniques at the higher frequencies for increased modal density. Due to the limited number of elements in the coupled FE/BE models, the validity of the deterministic results generated by the coupled FE/BE models at higher frequencies is uncertain.

5. CONCLUSIONS

Numerical models for nested cylindrical shells consisting of two cylindrical shells submerged in water and filled with water or air in the annular space between the shells have been presented. The cylinders are closed at each end by circular end plates. A fully coupled finite element/boundary element model of the fluid-loaded cylindrical shells was developed using MSC/Patran/Nastran and SYSNOISE. Several influencing factors corresponding to flexibility of the end plates, annular ribs coupling the cylindrical shells, heavy or light entrained fluid and non-concentricity of the cylindrical shells were investigated. A hybrid FE-SEA model of the nested cylindrical shells was also developed to examine the radiated sound power at higher frequencies. A reasonable agreement in the trend for the radiated sound power obtained deterministically and statistically was observed.

ACKNOWLEDGEMENT

The first author gratefully acknowledges the financial assistance provided by the Australian Acoustical Society NSW Division to attend the Inter-Noise 2014 conference.

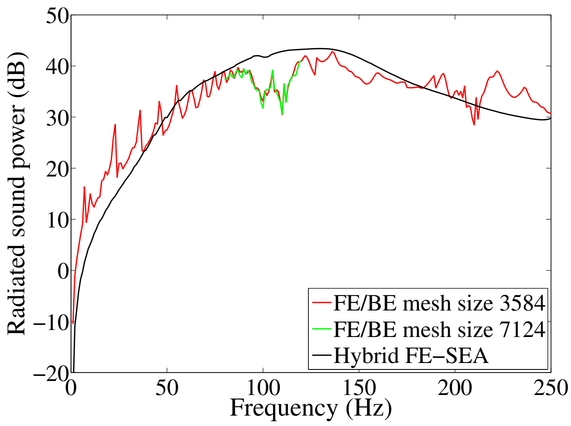

Figure 12 – Radiated sound power from the nested cylindrical shells without annular ribs

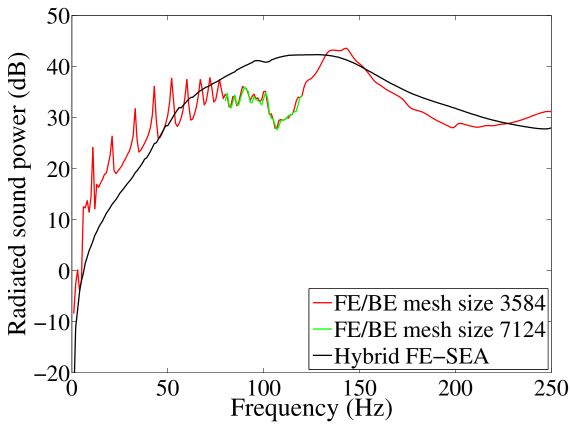

Figure 13 – Radiated sound power from the nested cylindrical shells with annular ribs

REFERENCES

1. Junger MC. Approaches to acoustic fluid-elastic structure interactions. J Acoust Soc Am. 1987;82(4):1115–1121.

2. Junger M, Feit D. Sound, Structures and Their Interaction. MIT Press; 1985.

3. Mackerle J. Fluid–structure interaction problems, finite element and boundary element approaches: A bibliography (1995–1998). Finite Elem An Des. 1999;31(3):231–240.

4. Caresta M, Kessissoglou N. Vibration of a submarine hull under harmonic propeller-shaft excitation. The Journal of the Acoustical Society of America. 2008;123(5):3062–3062.

5. Peters H, Kessissoglou N, Marburg S. Modal decomposition of exterior acoustic-structure interaction problems with model order reduction. The Journal of the Acoustical Society of America. 2014;135(5):2706–2717.

6. Lee JH, Kim J. Analysis and measurement of sound transmission through a double-walled cylindrical shell. J Sound Vib. 2002;251(4):631–649.

7. Skelton E. Acoustic scattering by a disk or annulus linking two concentric cylindrical shells, Part I: Theory and results for heavy exterior fluid loading. J Sound Vib. 1992;154(2):205–220.

8. Skelton E. Acoustic scattering by a disk or annulus linking two concentric cylindrical shells, Part II: Results for heavy exterior fluid loading on both shells. J Sound Vib. 1992;154(2):221–248.

9. Balena F, Prydz R, Revell J. Single- and double-wall cylinder noise reduction. J Aircraft. 1983;20(4):434–439.

10. Yoshikawa S. Fluid-structure coupling by the entrained fluid in submerged concentric double-shell vibration. J Acoust Soc Am. 1993;14(2):99–111.

11. Yoshikawa S, Williams EG, Washburn KB. Vibration of two concentric submerged cylindrical shells coupled by the entrained fluid. J Acoust Soc Am. 1994;95(6):3273–3286.

12. Lyon RH, DeJong RG. Theory and Applications of Statistical Energy Analysis. 2nd ed. Butterworth-Heinemann, Boston; 1995.

13. Langley RS, Bremner P. A hybrid method for the vibration analysis of complex structural-acoustic systems. J Acoust Soc Am. 1999;105(3):1657–1671.

14. Shorter PJ, Langley RS. Vibro-acoustic analysis of complex systems. J Sound Vib. 2005;288(3):669–699.

15. Bathe K. Finite Element Procedures in Engineering Analysis. Prentice Hall, Englewood Cliffs, New Jersey; 1982.

16. Craig R. Structural Dynamics: An Introduction to Computer Methods. John Wiley and Sons, Inc. New York; 1981.

17. Shin YS, Ham I. Damping modeling strategy for naval ship system. Monterey, CA 93943-5000: Naval Postgraduate School; 2003.

18. SYSNOISE Rev. 5.6, Users Manual. LMS International, Leuven, Belgium; 2003.

19. Fahy FJ, Gardonio P. Sound and Structural Vibration: Radiation, Transmission and Response. 2nd ed. Academic Press, Oxford; 2007.

20. VA One 2012 Users Guide, ESI Group. Paris, France; 2012.

21. Shaw RP. Radiation from a submerged elastic shell defined by nonconcentric cylinders. J Acoust Soc Am. 1978;64(1):311–317.